



Effects of inorganic oxidants on kinetics and mechanisms of WO_3 -mediated photocatalytic degradation



Heechan Kim ^{a,1}, Ha-Young Yoo ^{a,b,1}, Seokwon Hong ^a, Sanghyeop Lee ^{a,b}, Seunghak Lee ^{a,b}, Baek-Soo Park ^c, Hyunwoong Park ^d, Changha Lee ^e, Jaesang Lee ^{f,*}

^a Center for Water Resource Cycle, Korea Institute of Science and Technology (KIST), Seoul 136-791, Republic of Korea

^b Energy Environmental Policy and Technology, Green School, Korea University-KIST, Seoul 136-701, Republic of Korea

^c Korea National Cleaner Production Center, Korea Institute of Industrial Technology (KITECH), Seoul 135-918, Republic of Korea

^d Energy Engineering, Kyungpook National University, Daegu, 702-701, Republic of Korea

^e Urban and Environmental Engineering, and KIST-UNIST-Ulsan Center for Convergent Materials (KUUC), Ulsan National Institute of Science and Technology (UNIST), Ulsan 698-805, Republic of Korea

^f Civil, Environmental, and Architectural Engineering, Korea University, Seoul 136-701, Republic of Korea

ARTICLE INFO

Article history:

Received 17 April 2014

Received in revised form 30 June 2014

Accepted 7 July 2014

Available online 15 July 2014

Keywords:

Photocatalytic oxidation

Inorganic oxidant

Alternative electron acceptor

Charge separation

Visible light activity

ABSTRACT

This study evaluates the capacity of various inorganic oxidants (IO_4^- , HSO_5^- , $\text{S}_2\text{O}_8^{2-}$, H_2O_2 , and BrO_3^-) to act as alternative electron acceptors for WO_3 -mediated photocatalytic oxidation. Combination with IO_4^- drastically increased the rate of photocatalytic degradation of 4-chlorophenol by WO_3 , while the other oxyanions only negligibly improved the photocatalytic activity. The extent of the photocatalytic performance enhancement in the presence of inorganic oxidants correlated well with the efficiencies for: (1) hydroxylation of benzoic acid as an OH^* probe, (2) dechlorination of dichloroacetate as a hole scavenger, and (3) water oxidation with O_2 evolution. The results suggest that the promoted charge separation primarily causes kinetic enhancement in photocatalytic degradation using the $\text{WO}_3/\text{IO}_4^-$ system. In marked contrast to the substrate-dependent activity of the photochemically activated IO_4^- (generating selective IO_3^*), the efficiency of the $\text{WO}_3/\text{IO}_4^-$ system for photocatalytic degradation did not sensitively depend on the type of target organic compound, which implies the existence of a minor contribution of the photocatalytic reduction pathway associated with the production of IO_3^* as a secondary oxidant. On the other hand, the insignificant inhibitory effect of methanol as an OH^* quencher may reveal the possible involvement of SO_4^{2-} in the improved photocatalytic activity of the $\text{WO}_3/\text{HSO}_5^-$ system. The alternative use of platinized WO_3 , where the interfacial electron transfer occurs in a concerted step, achieved a highly accelerated photocatalytic oxidation in the presence of HSO_5^- and polyoxometalates as electron scavengers. In particular, the surface loading of nanoscale platinum appeared to retard the reaction route for SO_4^{2-} generation associated with a one-electron transfer.

© 2014 Elsevier B.V. All rights reserved.

1. Introduction

Photocatalysis using metal oxide semiconductors such as TiO_2 , ZnO , and WO_3 enables the generation of reactive oxidants (e.g., hydroxyl radical (OH^*)) and the associated degradation of organic compounds, providing a potential alternative to photochemical

advanced oxidation processes (e.g., O_3/UV and $\text{H}_2\text{O}_2/\text{UV}$) [1–4]. Key strategies to improve the TiO_2 - and ZnO -based photocatalytic systems in terms of energy usage involve extending the photoresponse to the visible light region, which is achieved by incorporating dopants [5,6], surface loading of plasmonic metals [7], and anchoring of organic photosensitizers [8,9]. Such modified photocatalysts are readily activated with visible light; at the same time, they allow the destruction of a limited group of organic compounds because the visible light activity is not associated with the photosensitization of nonselective OH^* [1,10,11]. On the other hand, valence band (VB) potential (+3.1 V_{NHE}) and band-gap energy (2.6 eV) of WO_3 appear to meet the criteria for visible light induced production of OH^* [4]. However, the energy level of the conduction band (CB) (+0.4 V_{NHE}) is not negative enough to employ

Abbreviations: CB, conduction band; DCA, dichloroacetic acid; EDS, energy dispersive X-ray spectrometer; IEP, isoelectric point; POM, polyoxometalate; TCD, thermal conductivity detector; VB, valence band.

* Corresponding author. Tel.: +82 2 3290 4864; fax: +82 2 928 7656.

E-mail address: lee39@korea.ac.kr (J. Lee).

¹ These authors contributed equally to this work.

O_2 as an electron acceptor, which results in a negligible apparent photocatalytic oxidation by WO_3 . As a result, the reaction route to scavenge CB electrons and facilitate the electron transfer at the semiconductor/water interface is critical to the visible light responsive activity of WO_3 .

Strategies that allow significant photocatalytic oxidation on WO_3 in the visible light region include: (1) use of alternative electron acceptors (e.g., Cu^{2+} , Fe^{3+} , H_2O_2) [12–15], (2) coupling of semiconductors with desirable band-gap structures [14,16–18], and (3) surface loading of cocatalysts (e.g., Pt, Pd, CuO) [1,4,19–21]. As the enhanced charge separation in the presence of Cu^{2+} led to a drastic acceleration in the WO_3 -mediated methanol oxidation [12], using either Fe^{3+} or H_2O_2 as an electron scavenger improved the photocatalytic activity of WO_3 for the oxidative degradation of 4-chlorophenol (4-CP) [13]. In particular, the synergistic combination of WO_3 with a Fenton-like reagent caused rapid degradation of various organic compounds, which is primarily ascribed to the increased efficiency of the Fenton process through the catalytic cycle of Fe^{2+}/Fe^{3+} [13]. Compositing with a semiconductor with an appropriate electronic structure and band gap also achieves a significant suppression of charge recombination in WO_3 [14,16,18]. Chatchai et al. [17] demonstrated that the efficient separation of photogenerated electron–hole pairs at the $WO_3/BiVO_4$ interface enhanced the oxidizing capacity of the coupled photocatalytic system. Consecutive reduction of O_2 on Pt-loaded WO_3 resulted in the effective production of OH^\bullet under visible light irradiation, which implies that surface deposition of cocatalysts allows WO_3 to utilize O_2 as a quencher of CB electrons through multielectron transfer [4,19]. Similarly, WO_3 surface modified with Pd and CuO exhibited highly improved activity for generating OH^\bullet relative to pure WO_3 , and outperformed nitrogen-doped TiO_2 for visible light induced mineralization of aldehyde and toluene [20,21].

It is well recognized that oxyanion oxidants, including bromate (BrO_3^-), hydrogen peroxide (H_2O_2), peroxymonosulfate (HSO_5^-), peroxydisulfate ($S_2O_8^{2-}$), and periodate (IO_4^-), cause kinetic retardation in the recombination of charge carriers in TiO_2 , enhancing the photocatalytic oxidation of organic substrates on the catalyst surface [22–24]. Addition of HSO_5^- , $S_2O_8^{2-}$, and IO_4^- led to a marked acceleration in photocatalytic oxidative degradation, which involves: (1) CB electron scavenging by the inorganic oxidants, and (2) photochemical activation of the oxyanions to produce numerous reactive intermediates such as O_3 , OH^\bullet , iodyl radical (IO_3^\bullet), and sulfate radical (SO_4^\bullet) [23–25]. The improvement in the photocatalytic performance is expected to be more pronounced for WO_3 in conjunction with inorganic oxidants, because electron acceptors apart from O_2 (henceforth, alternative electron acceptors) are indispensable for WO_3 -mediated photocatalytic oxidation. In particular, it is probable that WO_3 sensitizes the production of oxidizing intermediates because of the transfer of a CB electron to HSO_5^- , $S_2O_8^{2-}$, and IO_4^- under visible light irradiation, which could enable an energy efficient process compared to the photo-activation of oxyanions that is limited to operation with short wavelength UV [25–27].

This study explores the capability of various inorganic oxidants (IO_4^- , HSO_5^- , $S_2O_8^{2-}$, H_2O_2 , and BrO_3^-) as alternative electron acceptors to improve the photocatalytic activity of WO_3 for the oxidative degradation of 4-CP. The extent of the photocatalytic performance enhancement in the presence of inorganic oxidants is correlated with the efficiency of the combined WO_3 /inorganic oxidant systems for: (1) hydroxylation of benzoic acid (i.e., OH^\bullet production), (2) dechlorination of dichloroacetic acid (DCA) as a hole scavenger, and (3) O_2 generation by visible light induced water splitting. The effects of the reaction parameters (e.g., oxyanion dose and pH) on the kinetic rate of photocatalytic degradation of 4-CP are evaluated with WO_3 in conjunction with HSO_5^- , $S_2O_8^{2-}$, and IO_4^- . We also compare the efficiency of WO_3 combined with

HSO_5^- and IO_4^- for the photocatalytic degradation of a broad range of organics in the presence and absence of methanol as a scavenger for VB holes and OH^\bullet , which identifies the possible involvement of sulfur- or iodine-containing radical species in oxidative degradation. Surface-platinized WO_3 that initiates a multielectron transfer is examined for the photocatalyzed oxidation of 4-CP in the presence of oxyanion oxidants in order to promote their capacities as CB electron quenchers and secondary radical precursors.

2. Materials and methods

2.1. Reagents

The chemicals that were used as received include: titanium dioxide (TiO_2 , Degussa P25), tungsten oxide (WO_3 , nanopowder, Aldrich), chloroplatinic acid hydrate (Aldrich), benzoic acid (Sigma–Aldrich), bisphenol A (Aldrich), carbamazepine (Sigma–Aldrich), 4-chlorophenol (Aldrich), nitrobenzene (Sigma–Aldrich), sulfamethoxazole (Fluka), 2,4,6-trichlorophenol (Aldrich), hydrogen peroxide solution (30 wt% in H_2O , Sigma–Aldrich), sodium bromate (Sigma–Aldrich), sodium periodate (Sigma–Aldrich), OXONE® monopersulfate compound (Sigma–Aldrich), potassium peroxodisulfate (Sigma–Aldrich), phosphomolybdc acid hydrate ($H_3PMo_{12}O_{40}$ (abbreviated as PMo_{12}^{3-}), Sigma–Aldrich), phosphotungstic acid hydrate ($HNa_2PW_{12}O_{40}$ (abbreviated as PW_{12}^{3-}), Sigma–Aldrich), tungstosilicic acid hydrate ($H_4SiW_{12}O_{40}$ (abbreviated as SiW_{12}^{4-}), Aldrich), methanol (Sigma–Aldrich), perchloric acid (Sigma–Aldrich), sodium hydroxide (Fluka), phosphoric acid (Aldrich), and acetonitrile (J.T. Baker). Ultrapure deionized water (18 $M\Omega\text{ cm}$) prepared with a Millipore system was used. All chemicals were of reagent grade and used without further purification.

2.2. Characterization of WO_3 nanoparticles

The morphological analysis of WO_3 using a JEOL JEM 2100F high-resolution transmission electron microscope (HR-TEM) (Fig. 1a and b) confirmed that the primary particles, with sizes ranging from 50 to 100 nm, were typically spherical and formed clusters in aqueous solution. Elemental mapping using an energy dispersive X-ray spectrometer (EDS) (Fig. 1d and e) showed a uniform distribution of W and O on the entire surface of pristine WO_3 .

2.3. Photocatalytic experiments

Typical photocatalytic reactions were performed in a magnetically stirred cylindrical quartz reactor equipped with a 4-W fluorescent lamp (Philips Co.) under air-equilibrated conditions at ambient temperature ($22 \pm 1^\circ\text{C}$). A 4-W black light blue lamp (Philips Co.) was used to subject the photocatalytic systems to UV-A irradiation. The incident light intensity of the fluorescent lamp and of the black light blue lamp was measured using a pyranometer (Apogee, PYR-P) and determined to be 1.105 mW/cm^2 and 0.7 mW/cm^2 , respectively. A SpectroPro-500 spectrophotometer (Acton Research Co.) was used to record the emission spectral profiles (Supplementary Data, Fig. S1). The fluorescent lamp covers a relatively broad wavelength range of 350–650 nm, whereas the emission of the black light blue lamp spans the wavelength range of 350–400 nm. Experiments to examine the visible light activity of the WO_3 /oxyanion systems were conducted using a fluorescent lamp with a UV cut-off filter that was transmissive above 400 nm.

Typical reaction suspensions consisted of 0.5 g/L of WO_3 , 1 mM inorganic oxidant, and 0.1 mM target organic compound. The initial pH of the suspensions was adjusted to a desired value with 1 M $HClO_4$ or 1 M $NaOH$ solution. Aliquots of 1 mL samples

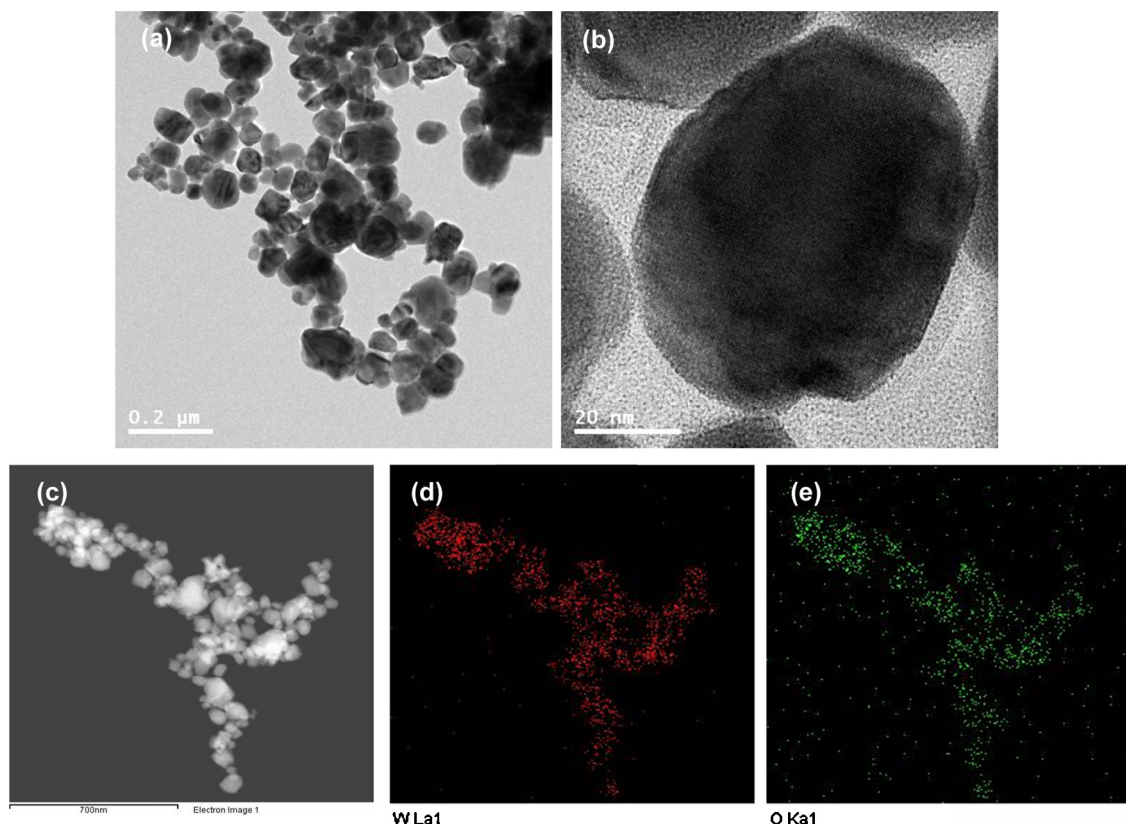


Fig. 1. Representative HR-TEM images of (a)–(b) pure WO_3 and (c) TEM image of WO_3 with the elemental maps, and the corresponding TEM/EDS maps of (d) tungsten and (e) oxygen. Red and green dots in the elemental maps represent tungsten and oxygen, respectively. (For interpretation of the references to color in this figure legend, the reader is referred to the web version of the article.)

at predetermined intervals of time were withdrawn from the photo-illuminated reactor using a 1 mL syringe, filtered through a 0.45- μm PTFE filter (Millipore), and transferred into a 2 mL amber glass vial. Experiments were conducted at least three times for any given condition. The residual concentrations of the target organic contaminants and iodine-containing substrates, including iodide (I^-), iodate (IO_3^-), and IO_4^- , were monitored using an HPLC (Shimadzu LC-20AD) equipped with a C-18 column (ZORBAX Eclipse XDB-C18) and UV/vis detector (Shimadzu SPD-20AV). The typical eluent comprised a binary mixture of 0.1% (v/v) phosphoric acid aqueous solution and acetonitrile (typically 70:30 v/v). Quantitative analyses of ionic intermediates, including BrO_3^- , SO_4^{2-} , Br^- , and Cl^- , were conducted using an ion chromatograph (IC, Dionex DX-120) equipped with Dionex IonPac AS-14 for anion detection and a conductivity detector. The residual concentrations of HSO_5^- and $\text{S}_2\text{O}_8^{2-}$ were determined colorimetrically [28].

2.4. Quantification of OH radical

Benzoic acid was selected as the probe compound in order to detect the photo-generated OH^\bullet [29]. The photocatalytic reactions proceeded in the presence of an excess amount of the chemical probe (i.e., 10 mM benzoic acid), which ensured that all OH radicals formed during the photo-irradiation of the WO_3 /inorganic oxidant systems were completely scavenged. The quantification of *p*-hydroxybenzoic acid generated by the photocatalytic hydroxylation of benzoic acid was performed using the HPLC.

2.5. Monitoring of O_2 evolution during photocatalytic water oxidation

Aqueous WO_3 suspensions (0.5 g/L, 30 mL) at pH 4 with or without inorganic oxidants (10 mM) were magnetically stirred in a

pyrex-glass reactor equipped with a quartz disc for irradiation. Prior to photo-irradiation using the simulated solar visible light (AM 1.5G; 150 mW/cm²; $\lambda > 420 \text{ nm}$), N_2 gas (99.9%) was purged through the suspension for 1 h, and the reactor was sealed from ambient air during the photolytic experiments. O_2 in the intermittently sampled headspace gas was quantitatively analyzed using a gas chromatograph (Young Lin, ACME 6100) equipped with a thermal conductivity detector (TCD) and molecular sieve (0.5 nm) column.

2.6. Preparation of platinized WO_3 photocatalysts

Surface-platinized WO_3 (Pt/WO_3) was prepared and characterized according to our previously published procedure [1,13]. An aqueous suspension of 0.5 g/L of WO_3 , containing 1 M methanol (electron donor) and 0.1 mM chloroplatinic acid, was irradiated with a 200-W mercury lamp for 30 min. After this photo-illumination that was conducted to cause irreversible deposition of platinum on the WO_3 surface was complete, Pt/WO_3 powder was separated from the resultant suspension using a 0.45 μm membrane filter, washed with Milli-Q water, and dried at 60 °C in a thermostat oven. Quantification of the platinum present in the initial aqueous WO_3 suspension and in the filtrate solution after the photodeposition was conducted to determine a typical Pt loading as ca. 0.5 wt%.

3. Results and discussion

3.1. Enhancement in photocatalytic activity of WO_3 in combination with inorganic oxidants

Fig. 2a and **b** demonstrate the photocatalytic oxidation of 4-CP by WO_3 in conjunction with various inorganic oxidants (BrO_3^- ,

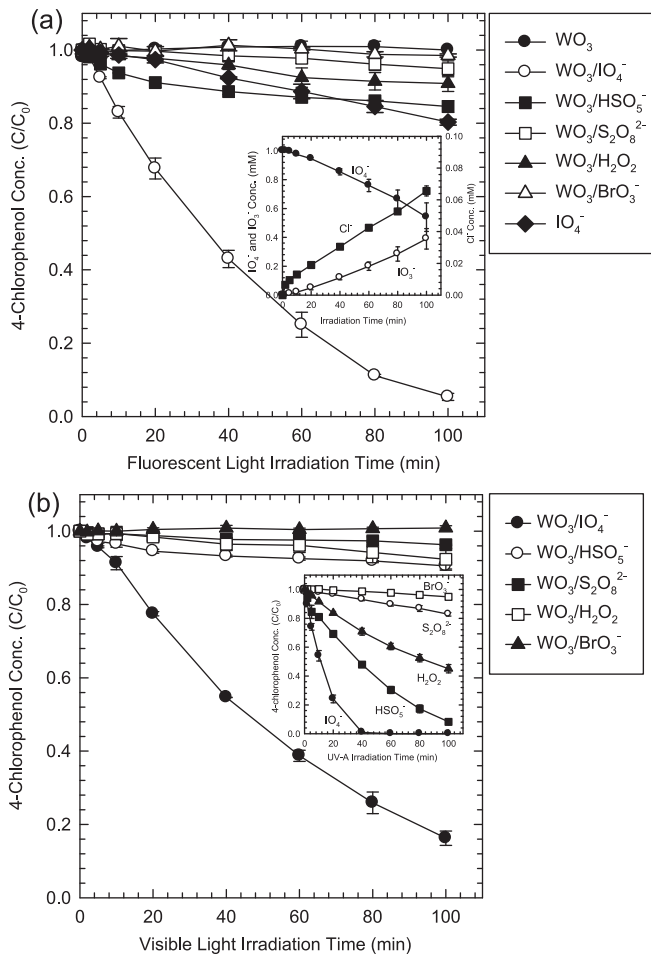


Fig. 2. Photocatalytic degradation of 4-CP by WO₃ in combination with IO₄⁻, HSO₅⁻, S₂O₈²⁻, H₂O₂, and BrO₃⁻ under irradiation of (a) fluorescent light (Inset: reductive conversion of IO₄⁻ into IO₃⁻ and production of Cl⁻) and (b) visible light (Inset: photocatalytic activity of the WO₃/oxyanion systems under UV-A light illumination) ([WO₃]₀ = 0.5 g/L; [inorganic oxidant]₀ = 1 mM; [4-CP]₀ = 0.1 mM; pH_i = 4.0).

H₂O₂, HSO₅⁻, S₂O₈²⁻, and IO₄⁻) under fluorescent and visible light irradiation. The pH of the suspensions was initially adjusted to 4.0, which changed negligibly during the photocatalytic reactions. Sorption in dark and direct photolysis did not cause any detectable reduction in the concentration of 4-CP (data not shown). WO₃ alone is capable of only negligible photocatalytic degradation of 4-CP, which assures the inability to employ O₂ as an electron acceptor in this system [4,13]. Although most of the oxyanions did not increase the photocatalytic activity of WO₃, their combination with IO₄⁻ drastically accelerated the photocatalyzed degradation of 4-CP under fluorescent light irradiation (Fig. 2a), which was accompanied by the corresponding evolution of chloride ions (inset of Fig. 2a). In contrast to the UV-A irradiation that photochemically activated IO₄⁻ to cause significant 4-CP degradation (Supplementary Data, Fig. S2) [25,27], the photosensitized oxidation proceeded marginally under fluorescent light illumination (Fig. 2a), which implies that the electron accepting capability of IO₄⁻ is crucial for the oxidizing power of the combined WO₃–IO₄⁻ system. The extent of improvement in the photocatalytic performance in the presence of inorganic oxidants correlated well with the efficiency of reductive conversion of oxyanions: the stoichiometric formation of IO₃⁻ from IO₄⁻ was efficiently performed on WO₃ (inset of Fig. 2a), while the reduction of other inorganic oxidants via CB electron was insignificant (Supplementary Data, Fig. S3). The WO₃/IO₄⁻ system for the photocatalytic degradation of 4-CP was still effective under

visible light irradiation ($\lambda > 400$ nm), with $k = 1.32 \pm 0.042 \text{ h}^{-1}$ for fluorescent light and $k = 1.03 \pm 0.024 \text{ h}^{-1}$ for visible light (Fig. 2b).

The superior activity of IO₄⁻ as an electron scavenger relative to other oxyanions was similarly confirmed by monitoring the rates of photocatalytic 4-CP degradation in the TiO₂/inorganic oxidant systems under fluorescent light irradiation (Supplementary Data, Fig. S4). Although only IO₄⁻ enabled a kinetic acceleration in photocatalyzed 4-CP oxidation (Supplementary Data, Fig. S4), previous studies demonstrated that the presence of HSO₅⁻ and S₂O₈²⁻ also improved the photocatalytic activity of semiconductors (e.g., TiO₂ and ZnO) to a significant extent for oxidative degradation [23,24]. The conflicting observations should mostly be attributable to a difference in the emission spectrum of the applied light source (Supplementary Data, Fig. S1). Under photo-irradiation with short-wavelength UV light, where intramolecular electron transfer in selected inorganic oxidants is achievable (Reactions (1)–(3)), oxidative pathways involving photochemically produced reactive oxidizing intermediates (e.g., OH[•], IO₃[•], and SO₄²⁻) proceed in parallel with the photocatalytic degradation by the semiconductor/inorganic oxyanion systems [23–25,27].



Additionally, because the alternative use of UV light favors the photo-induced electron transfer, the extent of enhancement in the photocatalytic performance in the presence of oxyanions should be more pronounced under UV irradiation. The inset of Fig. 2b shows that the efficiency of WO₃ for the photocatalyzed degradation of 4-CP noticeably increases in the presence of HSO₅⁻ and H₂O₂ under UV-A illumination. The negligible decomposition of 4-CP in the UV-A irradiated solutions of inorganic oxidants (except IO₄⁻) (Supplementary Data, Fig. S2) confirms the improved capacity of HSO₅⁻ and H₂O₂ as electron acceptors in WO₃ photocatalysis.

3.2. Effects of oxyanion dose and initial pH

Fig. 3a demonstrates the pseudo first order rate constants for photocatalytic 4-CP degradation as a function of the initial concentrations of selected inorganic oxidants, including IO₄⁻, HSO₅⁻, and S₂O₈²⁻. In accordance with the high capability of IO₄⁻ to promote the oxidative power of the WO₃ system (Fig. 2), the photocatalytic degradation efficiency was drastically enhanced when the initial dose of IO₄⁻ is increased, approaching a maximum when the IO₄⁻ concentration increased to 2.5–5.0 mM. A gradual increase in the initial concentration of HSO₅⁻ led to a moderate acceleration in the kinetics of photocatalyzed degradation of 4-CP, which implies that the alternative use of HSO₅⁻ as an electron acceptor enables charge separation in the WO₃ photocatalyst to a certain extent. On the other hand, the photocatalytic oxidation of 4-CP by the WO₃/S₂O₈²⁻ system was not significant until the initial concentration of S₂O₈²⁻ was increased to 5 mM.

Fig. 3b shows the effect of the initial pH on the kinetics of photocatalytic degradation of 4-CP by WO₃ in conjunction with IO₄⁻, HSO₅⁻, and S₂O₈²⁻. Acidic pH conditions favored the photocatalyzed 4-CP degradation by the WO₃/IO₄⁻ system, while oxidative 4-CP degradation was kinetically retarded at both neutral and alkaline pH. Because I(VII) speciation shifts from IO₄⁻ to H₂I₂O₁₀⁴⁻ with increasing pH [27], the reduced efficiency for 4-CP oxidation is likely attributed to electrostatic repulsion at higher pH (the isoelectric point (IEP) of WO₃ is observed at pH 2 [4]), which is detrimental to the transfer of a CB electron to periodate at the WO₃/water interface. Whereas the negligible removal of 4-CP occurred in the photo-irradiated suspensions of WO₃/S₂O₈²⁻ irrespective of the

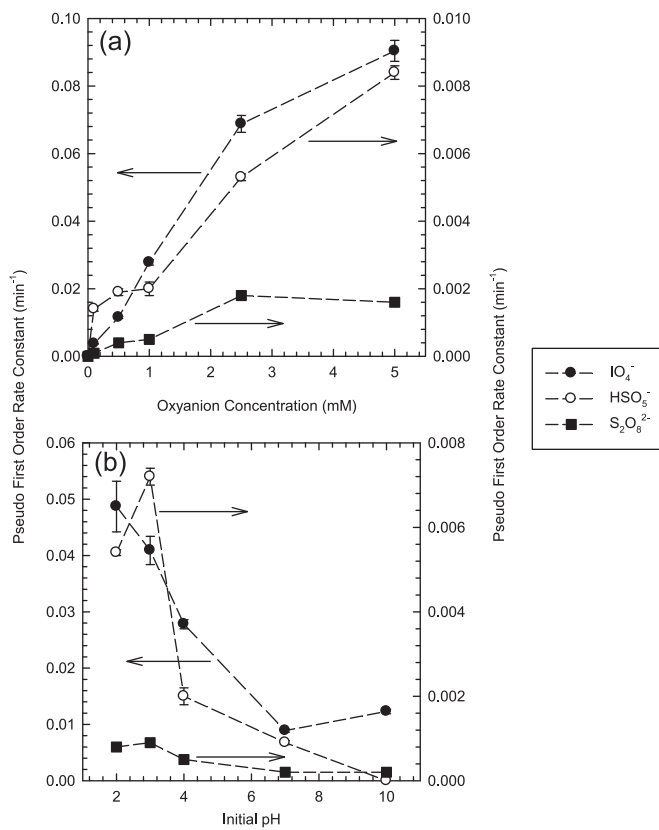


Fig. 3. Pseudo first-order rate constants for photocatalytic degradation of 4-CP by WO_3 in combination with IO_4^- , HSO_5^- , and $\text{S}_2\text{O}_8^{2-}$ as a function of (a) oxyanion dose ($[\text{WO}_3]_0 = 0.5 \text{ g/L}$; [inorganic oxidant]₀ = 0.1, 0.5, 1, 2.5, and 5 mM; [4-CP]₀ = 0.1 mM; $\text{pH}_i = 4.0$) and (b) initial pH ($[\text{WO}_3]_0 = 0.5 \text{ g/L}$; [inorganic oxidant]₀ = 1 mM; [4-CP]₀ = 0.1 mM; $\text{pH}_i = 2.0, 3.0, 4.0, 7.0$, and 10.0). The photolytic experiments were performed under fluorescent light irradiation.

initial pH, strong acidic conditions whereby WO_3 is positively charged allowed the $\text{WO}_3/\text{HSO}_5^-$ system to effectively decompose 4-CP. From the pK_a values ($\text{pK}_{a,1} = 0.5$ [30]; $\text{pK}_{a,2} = 9.3$ [31]), it can be concluded that peroxymonosulfate predominantly exists as an anionic species such as HSO_5^- and SO_5^{2-} over the pH range 2–10. Consequently, the favorable interaction with the positively charged WO_3 surface at a strong acidic pH enhances the interfacial electron transfer to HSO_5^- and the associated charge separation in WO_3 , eventually increasing the kinetic rate of photocatalytic oxidative degradation.

3.3. Comparison of electron accepting activity of inorganic oxidants

To evaluate the capacity of inorganic oxidants as electron scavengers to improve the charge-separation efficiency, we monitored the rate of OH^\bullet production from the WO_3 /inorganic oxyanion systems under fluorescent light irradiation. Fig. 4a shows that the presence of IO_4^- drastically increases the photocatalytic efficiency for the production of *p*-hydroxybenzoic acid (i.e., hydroxylation of benzoic acid is an indirect indication for OH^\bullet yield [29]), while the conversion was minor with the other oxyanions, including HSO_5^- , $\text{S}_2\text{O}_8^{2-}$, and BrO_3^- . As an alternative approach to identify the role of inorganic oxidants in charge separation, we compared the photocatalytic activity of WO_3 /oxyanion systems for oxidative degradation of DCA (i.e., rate of chloride-ion release by dechlorination) that contains no H atoms available for OH^\bullet -induced abstraction and is primarily oxidized via a VB hole [32]. Fig. 4b demonstrates that the photocatalytic oxidation of DCA as

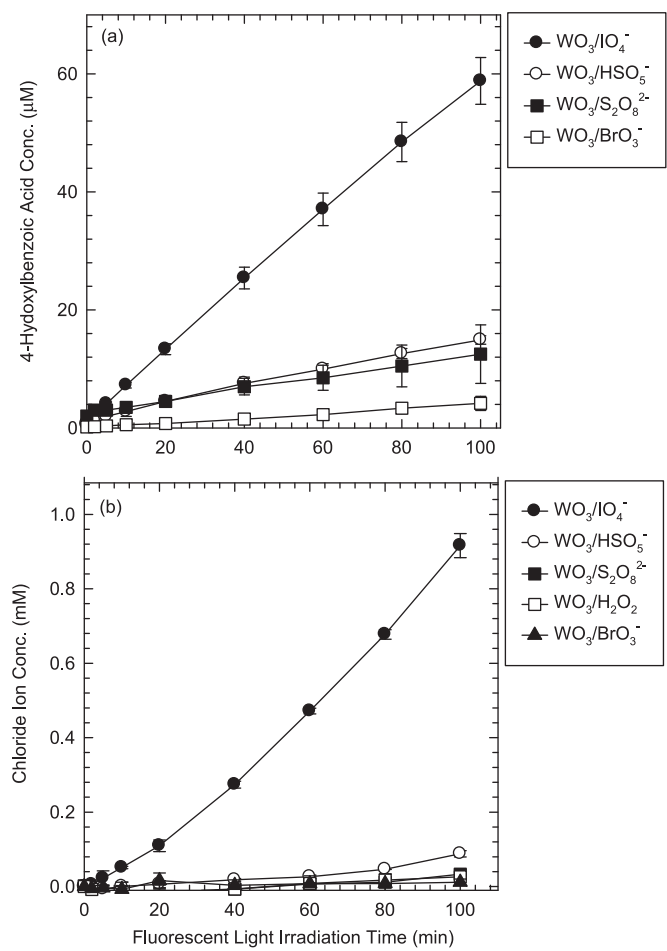


Fig. 4. (a) Production of *p*-hydroxybenzoic acid during photocatalytic oxidation of benzoic acid by WO_3 /oxyanion systems ($[\text{WO}_3]_0 = 0.5 \text{ g/L}$; [inorganic oxidant]₀ = 1 mM; [benzoic acid]₀ = 10 mM; $\text{pH}_i = 4.0$) and (b) evolution of chloride ion by photocatalytic dechlorination of dichloroacetate by WO_3 /oxyanion systems ($[\text{WO}_3]_0 = 0.5 \text{ g/L}$; [inorganic oxidant]₀ = 1 mM; [dichloroacetate]₀ = 10 mM; $\text{pH}_i = 4.0$). The photolytic experiments were performed under fluorescent light irradiation.

a hole scavenger was significant in the presence of IO_4^- , while WO_3 in conjunction with the other oxyanions negligibly degraded DCA under fluorescent light irradiation. The experiments that monitored the rate of O_2 evolution during visible light induced photocatalytic oxidation of water (mainly performed by photogenerated VB holes) also confirmed the higher capability of IO_4^- to enable an effective electron-hole separation relative to the other inorganic oxidants (Fig. 5). The superiority of HSO_5^- as an electron acceptor relative to $\text{S}_2\text{O}_8^{2-}$ seems to be more pronounced in the production of O_2 from water (Fig. 5) than in the photocatalytic degradation of 4-CP (Fig. 2a). This is because the photocatalytic oxidation of water was performed using an initial oxyanion concentration of 10 mM (note that the difference in photocatalytic efficiency between the $\text{WO}_3/\text{HSO}_5^-$ and $\text{WO}_3/\text{S}_2\text{O}_8^{2-}$ systems becomes more significant as the oxyanion concentration increases (Fig. 3a)). The slightly enhanced generation of O_2 in the presence of HSO_5^- indicates that it could more effectively quench the CB electrons compared to $\text{S}_2\text{O}_8^{2-}$, although the reduction potential of $\text{S}_2\text{O}_8^{2-}$ is more positive (i.e., $E^0(\text{HSO}_5^-/\text{HSO}_4^-) = +1.82 \text{ V}_{\text{NHE}}$ [33] versus $E^0(\text{S}_2\text{O}_8^{2-}/\text{HSO}_4^-) = +2.08 \text{ V}_{\text{NHE}}$ [34]). The combined results are compatible with the extent of the photocatalytic performance improvement (Fig. 2a), which implies that the enhanced charge separation/transfer processes through the combination with oxyanions, rather than the production of secondary oxidants

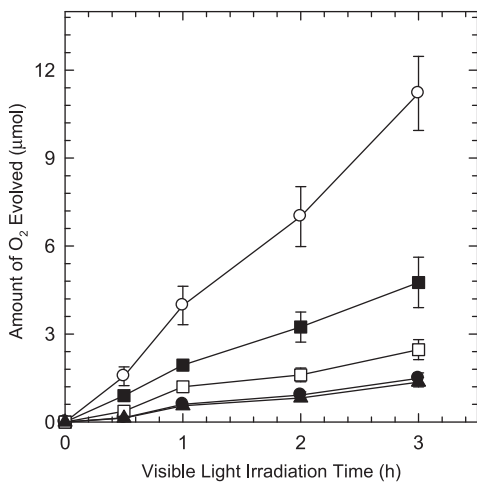
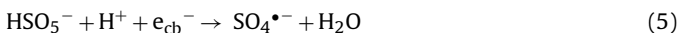
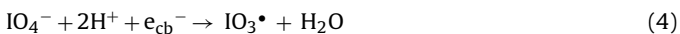


Fig. 5. Generation of oxygen during visible light induced photocatalytic oxidation of water by WO_3 /oxyanion systems ($[\text{WO}_3]_0 = 0.5 \text{ g/L}$; $[\text{inorganic oxidant}]_0 = 10 \text{ mM}$; $\text{pH}_i = 4.0$).

(IO_3^\bullet and SO_4^\bullet) by the reductive conversion of selected oxyanions (IO_4^- , HSO_5^- , and $\text{S}_2\text{O}_8^{2-}$) (Reactions (4) and (5)), primarily contribute to the photocatalytic activity of the WO_3 /inorganic oxidant systems.



3.4. Photocatalytic oxidative degradation of various organic contaminants

Fig. 6 compares the efficiencies of the $\text{WO}_3/\text{IO}_4^-$ and $\text{WO}_3/\text{HSO}_5^-$ systems for the photocatalytic oxidative degradation of diverse organic compounds under fluorescent light irradiation. Although HSO_5^- was applied at a fivefold higher concentration than IO_4^- , the $\text{WO}_3/\text{IO}_4^-$ system degraded the target substrates more

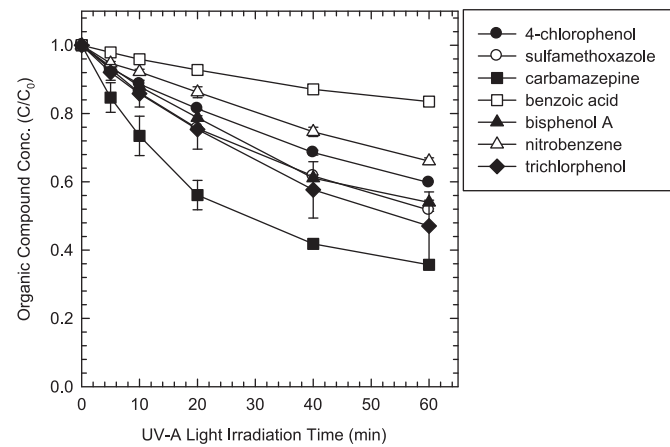


Fig. 7. Oxidative degradation of organic compounds by periodate that is photochemically activated with UV-A in the presence of methanol ($[\text{IO}_4^-]_0 = 1 \text{ mM}$; $[\text{benzoic acid}]_0 = [\text{bisphenol A}]_0 = [\text{4-CP}]_0 = [\text{nitrobenzene}]_0 = [\text{sulfamethoxazole}]_0 = [\text{trichlorophenol}]_0 = 0.1 \text{ mM}$; $[\text{carbamazepine}] = 0.05 \text{ mM}$; $[\text{methanol}]_0 = 20 \text{ mM}$; $\text{pH}_i = 4.0$).

rapidly than the $\text{WO}_3/\text{HSO}_5^-$ system, which assures the excellent activity of IO_4^- as an alternative electron acceptor. The efficiency of the $\text{WO}_3/\text{IO}_4^-$ system for photocatalyzed oxidation did not have a sensitive dependence on the type of target compound, and the presence of methanol as an OH^\bullet scavenger drastically retarded the kinetics of photocatalytic degradation of all target substrates (Fig. 6). On the other hand, photochemically activated IO_4^- in the presence of excess methanol (as a quencher of atomic oxygen ($\text{O}^{3\text{P}}$)) and OH^\bullet exhibited selective reactivity, because it exclusively produced IO_3^\bullet as a reactive intermediate [25]. Oxidative degradation of carbamazepine was significant, and some phenols (4-CP and bisphenol A) were decomposed at a moderate rate, while benzoic acid underwent slow destruction (Fig. 7). Our previous findings [35] showed that the substrate-dependent oxidizing capacity of the activated IO_4^- allowed significant degradation of phenolic compounds when excess OH^\bullet quenchers such as humic

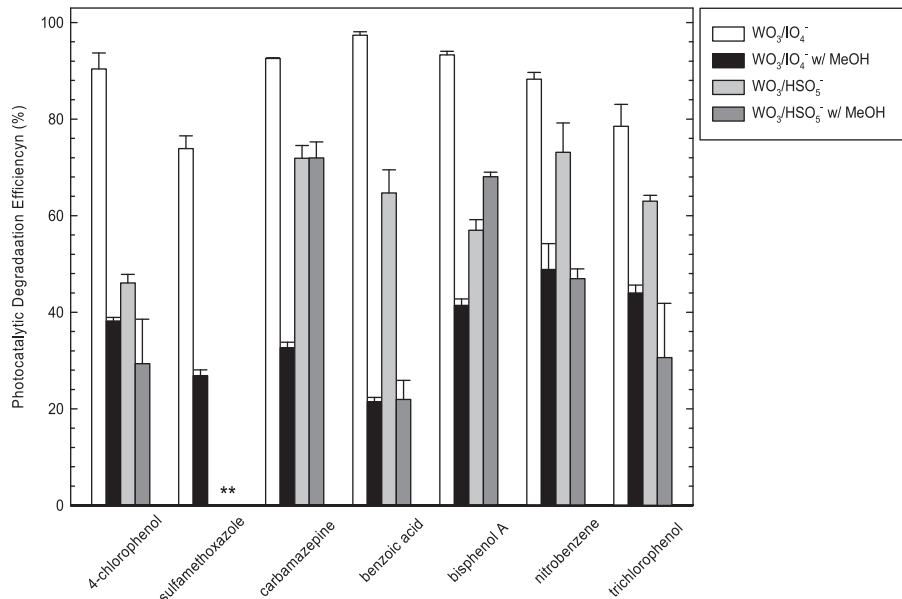


Fig. 6. Efficiencies of photocatalytic degradation of organic compounds by WO_3 in combination with IO_4^- and HSO_5^- in the presence and absence of methanol ($[\text{WO}_3]_0 = 0.5 \text{ g/L}$; $[\text{IO}_4^-]_0 = 1 \text{ mM}$; $[\text{HSO}_5^-]_0 = 5 \text{ mM}$; $[\text{benzoic acid}]_0 = [\text{bisphenol A}]_0 = [\text{4-CP}]_0 = [\text{nitrobenzene}]_0 = [\text{sulfamethoxazole}]_0 = [\text{trichlorophenol}]_0 = 0.1 \text{ mM}$; $[\text{carbamazepine}] = 0.05 \text{ mM}$; $[\text{methanol}]_0 = 20 \text{ mM}$; $\text{pH}_i = 4.0$); “**” indicates the failure to quantify the residual concentrations of sulfamethoxazole in the presence of excess HSO_5^- .

acid and *tert*-butanol were applied. Therefore, the negligible substrate specificity of the $\text{WO}_3/\text{IO}_4^-$ system and noticeable activity of methanol as a quencher combined imply a minor role of IO_3^\bullet as a secondary oxidant (possibly generated through the CB electron-induced reduction of IO_4^- (Reaction (4)), although previous studies have suggested the possible production of IO_3^\bullet from the photo-excited semiconductor/ IO_4^- system [22,25].

Whereas the nonselective nature of $\text{SO}_4^{\bullet-}$ enables the oxidative degradation of a wide spectrum of organic compounds, the reaction with methanol is kinetically slow compared to OH^\bullet -induced oxidation of methanol (i.e., $k(\text{methanol} + \text{SO}_4^{\bullet-}) = 3.2 \times 10^6 \text{ M}^{-1} \text{ s}^{-1}$ [36] versus $k(\text{methanol} + \text{OH}^\bullet) = 9.7 \times 10^8 \text{ M}^{-1} \text{ s}^{-1}$ [37]). Similar to the $\text{WO}_3/\text{IO}_4^-$ system, the photocatalytic activity of the $\text{WO}_3/\text{HSO}_5^-$ system is not substrate-dependent (Fig. 6). On the other hand, the efficiency assessment for the photocatalytic oxidation of diverse organics (Fig. 6) demonstrates that the reduction in the extent of performance in the presence of excess methanol was not significant in the $\text{WO}_3/\text{HSO}_5^-$ system relative to the $\text{WO}_3/\text{IO}_4^-$ system (e.g., the ratio of pseudo first order rate constants for photocatalytic degradation in the presence of methanol (k_{MEOH}) to that in the absence of methanol (k), $k_{\text{MEOH}}/k(\text{carbamazepine}) = 1.02$ for the $\text{WO}_3/\text{HSO}_5^-$ system versus 0.19 for the $\text{WO}_3/\text{IO}_4^-$ system). The results suggest that the enhanced photocatalytic activity of the $\text{WO}_3/\text{HSO}_5^-$ system could be ascribed in part to the production of $\text{SO}_4^{\bullet-}$ by the photocatalytic reduction of HSO_5^- on WO_3 (Reaction (5)).

3.5. Effect of surface platinization

Fig. 8a shows the role of inorganic oxidants in the photocatalytic degradation of 4-CP by Pt/WO_3 . Loading of platinum deposits on the surface of WO_3 initiates a new reaction route that allows a multielectron reduction of O_2 to generate OH^\bullet under visible light irradiation (i.e., $\text{O}_2 + 2\text{H}^+ + 2\text{e}_{\text{cb}}^- \rightarrow \text{H}_2\text{O}_2$; $\text{H}_2\text{O}_2 + \text{e}_{\text{cb}}^- \rightarrow \text{OH}^- + \text{OH}^\bullet$) [4]. Pt/WO_3 alone caused only a slight reduction in the 4-CP concentration under fluorescent light irradiation. When Pt/WO_3 was alternatively used as the photocatalyst instead of bare WO_3 , the enhancement in the photocatalytic efficiency was negligible when the combination of $\text{S}_2\text{O}_8^{2-}$ and BrO_3^- is used, and the addition of H_2O_2 even retarded the kinetic rate of 4-CP degradation by Pt/WO_3 (Fig. 8a). The inhibitory effect of H_2O_2 may be related to the catalytic conversion of H_2O_2 into O_2 by photodeposited platinum that exists in various oxidation states on WO_3 (dark reactions) [38,39], which initiates the reversible reduction/oxidation (redox) reactions of PtO (Pt^{II}) and PtO_2 (Pt^{IV}) (Reactions (6) and (7)) [39].



The $\text{Pt}^{\text{II}}/\text{Pt}^{\text{IV}}$ species that predominate under oxidizing conditions could act as a recombination center [40]. That is, the sequential redox cycles of $\text{Pt}^{\text{II}}/\text{Pt}^{\text{IV}}$ could consume significant amounts of photogenerated electrons and holes and prevent the charge carriers from contributing to the photocatalytic activity of Pt/WO_3 . On the other hand, surface platinization of WO_3 accelerated the photocatalytic degradation of 4-CP in the presence of IO_4^- and HSO_5^- (Fig. 8a). In particular, the improvement in the photocatalytic activity of Pt/WO_3 was more pronounced with HSO_5^- , which is in marked contrast to the slow oxidative degradation of 4-CP during the photo-illumination of the $\text{WO}_3/\text{HSO}_5^-$ system (i.e., degradation efficiency (after 100 min of photo-illumination) = $86.05 \pm 2.33\%$ for the $\text{Pt}/\text{WO}_3/\text{HSO}_5^-$ system versus $15.45 \pm 1.63\%$ for the $\text{WO}_3/\text{HSO}_5^-$ system). The ability of Pt/WO_3 to more readily employ HSO_5^- (or IO_4^-) as an electron

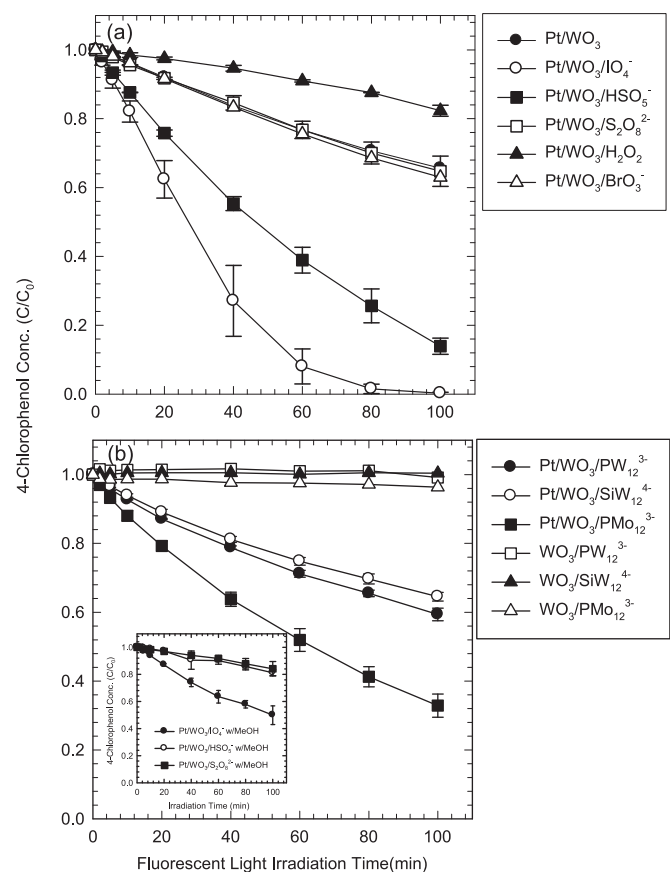


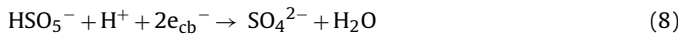
Fig. 8. Photocatalytic degradation of 4-CP by platinized WO_3 in combination with (a) inorganic oxidants and (b) polyoxometalates (Inset: photocatalytic oxidation of 4-CP by the $\text{WO}_3/\text{oxanion}$ systems in the presence of methanol) ($[\text{WO}_3]_0 = 0.5 \text{ g/L}$; $[\text{inorganic oxidant}]_0 = [\text{polyoxometalate}]_0 = 1 \text{ mM}$; $[4\text{-CP}]_0 = 0.1 \text{ mM}$; $[\text{methanol}]_0 = 20 \text{ mM}$; $\text{pH}_i = 4.0$).

scavenger was compatible with the accelerated conversion of HSO_5^- (or IO_4^-) into SO_4^{2-} (or IO_3^-) (data not shown).

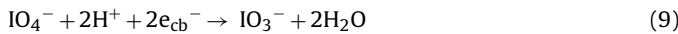
As metal-oxygen cluster anions, polyoxometalates (POMs) can undergo multi-electron transfer reactions with minimal structural changes [41], thereby acting as electron scavengers to improve the photocatalytic activity of TiO_2 [42]. Fig. 8b demonstrates that an increase in the photocatalytic degradation efficiency in the presence of POMs such as SiW_{12}^{4-} , PW_{12}^{3-} , and PMo_{12}^{3-} occurred exclusively on Pt/WO_3 , whereas POMs were ineffective as electron acceptors in aqueous suspensions of pure WO_3 . POM alone was not photoactive for the oxidative degradation of 4-CP under fluorescent light irradiation (data not shown). Because CB electron-mediated reduction of POMs is not associated with formation of secondary oxidizing intermediates, the results confirm the role of platinum deposits in the enhanced interfacial transfer of CB electrons to an electron acceptor. The most positive reduction potential (i.e., PMo_{12}^{3-} ($E^0 = +0.65 \text{ V}_{\text{NHE}}$) $> \text{PW}_{12}^{3-}$ ($E^0 = +0.218 \text{ V}_{\text{NHE}}$) $> \text{SiW}_{12}^{4-}$ ($E^0 = +0.054 \text{ V}_{\text{NHE}}$) [43]) likely allowed PMo_{12}^{3-} to more effectively capture the CB electrons and remove 4-CP compared to SiW_{12}^{4-} and PW_{12}^{3-} . Although one-electron reduction of SiW_{12}^{4-} (or PW_{12}^{3-}) is not thermodynamically favorable (note that the CB edge potential of WO_3 is $+0.4 \text{ V}_{\text{NHE}}$), the presence of SiW_{12}^{4-} (or PW_{12}^{3-}) improved the photocatalytic activity of Pt/WO_3 to a moderate extent (Fig. 8b), which implies that the transfer of a CB electron from the photo-excited Pt/WO_3 to SiW_{12}^{4-} (or PW_{12}^{3-}) could be performed in a concerted step involving multielectron transfer (e.g., $\text{SiW}_{12}^{4-} + 2\text{e}_{\text{cb}}^- \rightarrow \text{SiW}_{12}^{6-}$). Note that the surface platinization enables the two-electron reduction of oxygen on WO_3 , which

proceeds more favorably than the one-electron reduction in terms of reduction potentials (i.e., $E^0(\text{O}_2/\text{H}_2\text{O}_2) = +0.695 \text{ V}_{\text{NHE}}$ [44] versus $E^0(\text{O}_2/\text{O}_2^{\bullet-}) = -0.33 \text{ V}_{\text{NHE}}$ [45]).

In contrast to the insignificant inhibitory effect of methanol on the photocatalytic activity of the $\text{WO}_3/\text{HSO}_5^-$ system for 4-CP degradation (Fig. 6), the addition of excess methanol as an OH^\bullet scavenger drastically quenched the photocatalyzed oxidation by the $\text{Pt}/\text{WO}_3/\text{HSO}_5^-$ system (inset of Fig. 8b), which implies that surface deposition of nanosized Pt particles may hinder reductive conversion of HSO_5^- to $\text{SO}_4^{\bullet-}$. The switching of reaction pathways may suggest the possibility of a two-electron reduction reaction on Pt/WO_3 , where the availability of HSO_5^- as an electron acceptor is improved but the conversion into SO_4^{2-} , rather than $\text{SO}_4^{\bullet-}$ (Reaction (8)), is preferred.



On the other hand, the presence of methanol still considerably decreased the rate of photocatalytic 4-CP degradation in the presence of IO_4^- when Pt/WO_3 was alternatively employed. These results may indicate that both pure WO_3 and Pt/WO_3 enable the reduction of IO_4^- via a two-electron transfer process (Reaction (9)), which does not involve the production of IO_3^\bullet .



There is a need of further studies exploring the effect of metal cocatalysts on the photocatalytic activation of inorganic oxyanions (leading to production of inorganic radical intermediates), based on the multi-activity assessment of the combined Pt/WO_3 /oxyanion systems and spectroscopic monitoring of oxyanion-derived oxidizing radicals.

4. Conclusions

This study examined various inorganic oxidants as alternative electron acceptors for improving the photocatalytic activity of WO_3 . The presence of IO_4^- drastically accelerated WO_3 -mediated photocatalytic oxidation under fluorescent and visible light irradiation, which was in marked contrast to the minor contribution of other oxyanions (HSO_5^- , $\text{S}_2\text{O}_8^{2-}$, H_2O_2 , and BrO_3^-) as electron scavengers. When a fivefold higher concentration of HSO_5^- was applied, the $\text{WO}_3/\text{IO}_4^-$ system outperformed the $\text{WO}_3/\text{HSO}_5^-$ system in the photocatalyzed oxidation of 4-CP by a significant margin, which assures the superior capacity of IO_4^- as an electron acceptor. From the rates of: (1) hydroxylation of benzoic acid (indirect indication of OH^\bullet production), (2) dechlorination of DCA as a hole scavenger, and (3) O_2 generation by water oxidation, it is suggested that the role of IO_4^- in the enhanced photocatalytic degradation is primarily attributable to the effective charge separation in WO_3 photocatalysis rather than CB electron-induced conversion of IO_4^- into IO_3^\bullet . Whereas photochemically activated IO_4^- in the presence of methanol (exclusively producing IO_3^\bullet as the main oxidant) showed substrate-specific reactivity, the $\text{WO}_3/\text{IO}_4^-$ system effectively degraded a wide range of organic compounds, which assures that the ability of IO_4^- in facilitating the charge separation (leading to the promoted yield of an OH^\bullet (or a VB hole) as a nonselective oxidant) is critical to the accelerated photocatalytic degradation. Unlike the $\text{WO}_3/\text{IO}_4^-$ system that underwent a drastic decrease in the photocatalytic activity in the presence of excess methanol as an OH^\bullet scavenger, the $\text{WO}_3/\text{HSO}_5^-$ system still caused significant oxidative degradation of organic compounds (e.g., bisphenol A and carbamazepine) when methanol was added, which may suggest a possible degradation route initiated by $\text{SO}_4^{\bullet-}$ as a secondary oxidant (reductively produced from HSO_5^- via a CB electron). Surface modification with nanosized platinum particles enabled the multielectron transfer of WO_3 , and allowed for the use of selected

oxyanions (e.g., HSO_5^- , SiW_{12}^{4-} , PW_{12}^{3-} , and PMo_{12}^{3-}) as electron acceptors such that photocatalytic oxidation was kinetically enhanced to a significant extent.

Acknowledgments

This study was supported by the Korea Ministry of Environment as part of “The Converging Technology Project” (2012000600002) and by the KIST-UNIST partnership program (2.130404.01).

Appendix A. Supplementary data

Supplementary data associated with this article can be found, in the online version, at <http://dx.doi.org/10.1016/j.apcatb.2014.07.019>.

References

- [1] J. Choi, H. Lee, Y. Choi, S. Kim, S. Lee, S. Lee, W. Choi, J. Lee, *Appl. Catal. B Environ.* 147 (2014) 8–16.
- [2] M.J. Height, S.E. Pratsinis, O. Mekasuwandumrong, P. Praserthdam, *Appl. Catal. B Environ.* 63 (2006) 305–312.
- [3] M.R. Hoffmann, S.T. Martin, W.Y. Choi, D.W. Bahnemann, *Chem. Rev.* 95 (1995) 69–96.
- [4] J. Kim, C.W. Lee, W. Choi, *Environ. Sci. Technol.* 44 (2010) 6849–6854.
- [5] J. Choi, H. Park, M.R. Hoffmann, *J. Phys. Chem. C* 114 (2010) 783–792.
- [6] G.D. Yang, Z. Jiang, H.H. Shi, T.C. Xiao, Z.F. Yan, *J. Mater. Chem.* 20 (2010) 5301–5309.
- [7] E. Kowalska, R. Abe, B. Ohtani, *Chem. Commun.* (2009) 241–243.
- [8] T.X. Wu, G.M. Liu, J.C. Zhao, H. Hidaka, N. Serpone, *J. Phys. Chem. B* 102 (1998) 5845–5851.
- [9] G. Zhang, W.Y. Choi, *Chem. Commun.* 48 (2012) 10621–10623.
- [10] J. Lee, S. Hong, Y. Mackeyev, C. Lee, E. Chung, L.J. Wilson, J.H. Kim, P.J.J. Alvarez, *Environ. Sci. Technol.* 45 (2011) 10598–10604.
- [11] M. Mrowetz, W. Balcerski, A.J. Colussi, M.R. Hoffmann, *J. Phys. Chem. B* 108 (2004) 17269–17273.
- [12] T. Arai, M. Yanagida, Y. Konishi, A. Ikura, Y. Iwasaki, H. Sugihara, K. Sayama, *Appl. Catal. B Environ.* 84 (2008) 42–47.
- [13] H. Lee, J. Choi, S. Lee, S.T. Yun, C. Lee, J. Lee, *Appl. Catal. B Environ.* 138 (2013) 311–317.
- [14] T. Ohno, F. Tanigawa, K. Fujihara, S. Izumi, M. Matsumura, *J. Photochem. Photobiol. A Chem.* 118 (1998) 41–44.
- [15] Y. Nosaka, S. Takahashi, H. Sakamoto, A.Y. Nosaka, *J. Phys. Chem. C* 115 (2011) 21283–21290.
- [16] M.R. Bayati, F. Golestanian-Fard, A.Z. Moshfegh, *Appl. Catal. A. Gen.* 382 (2010) 322–331.
- [17] P. Chatchai, Y. Murakami, S.Y. Kishioka, A.Y. Nosaka, Y. Nosaka, *Electrochim. Acta* 54 (2009) 1147–1152.
- [18] T. Arai, M. Yanagida, Y. Konishi, Y. Iwasaki, H. Sugihara, K. Sayama, *J. Phys. Chem. C* 111 (2007) 7574–7577.
- [19] R. Abe, H. Takami, N. Murakami, B. Ohtani, *J. Am. Chem. Soc.* 130 (2008) 7780–7781.
- [20] Y.G. Liu, Y. Ohko, R.Q. Zhang, Y.N. Yang, Z.Y. Zhang, *J. Hazard. Mater.* 184 (2010) 386–391.
- [21] T. Arai, M. Horiguchi, M. Yanagida, T. Gunji, H. Sugihara, K. Sayama, *J. Phys. Chem. C* 113 (2009) 6602–6609.
- [22] S.T. Martin, A.T. Lee, M.R. Hoffmann, *Environ. Sci. Technol.* 29 (1995) 2567–2573.
- [23] C.K. Gratzel, M. Jirousek, M. Gratzel, *J. Mol. Catal.* 60 (1990) 375–387.
- [24] E. Pelizzetti, V. Carlini, C. Minero, M. Gratzel, *New J. Chem.* 15 (1991) 351–359.
- [25] L.H. Chia, X.M. Tang, L.K. Weavers, *Environ. Sci. Technol.* 38 (2004) 6875–6880.
- [26] S.Y. Yang, P. Wang, X. Yang, L. Shan, W.Y. Zhang, X.T. Shao, R. Niu, *J. Hazard. Mater.* 179 (2010) 552–558.
- [27] C. Lee, J. Yoon, *J. Photochem. Photobiol. A* 165 (2004) 35–41.
- [28] C.J. Liang, C.F. Huang, N. Mohanty, R.M. Kurakalva, *Chemosphere* 73 (2008) 1540–1543.
- [29] X.L. Zhou, K. Mopper, *Mar. Chem.* 30 (1990) 71–88.
- [30] H. Elias, U. Gotz, K.J. Wannowius, *Atmos. Environ.* 28 (1994) 439–448.
- [31] D.F. Evans, M.W. Upton, *J. Chem. Soc. Dalton Trans.* (1985) 1141–1145.
- [32] D.W. Bahnemann, M. Hilgendorff, R. Memming, *J. Phys. Chem. B* 101 (1997) 4265–4275.
- [33] W.V. Steele, E.H. Appelman, *J. Chem. Thermo.* 14 (1982) 337–344.
- [34] A.J. Bard, R. Parsons, J. Jordan, *Standard Potentials in Aqueous Solution*, Marcel Dekker, Inc, New York, Basel, 1985.
- [35] H. Lee, H.-Y. Yoo, I.-H. Nam, S. Lee, S. Lee, J.-H. Kim, C. Lee, J. Lee, *Environ. Sci. Technol.* (2014), in press.
- [36] H. Eibenberger, S. Steenken, P. O'Neill, D. Schultefrohlinde, *J. Phys. Chem.* 82 (1978) 749–750.

- [37] G.V. Buxton, C.L. Greenstock, W.P. Helman, A.B. Ross, *J. Phys. Chem. Ref. Data* 17 (1988) 513–886.
- [38] M. Kajita, K. Hikosaka, M. Iitsuka, A. Kanayama, N. Toshima, Y. Miyamoto, *Free Rad. Res.* 41 (2007) 615–626.
- [39] H. Okamoto, K. Horii, A. Fujisawa, Y. Yamamoto, *Exp. Dermatol.* 21 (2012) 5–7.
- [40] J. Lee, W. Choi, *J. Phys. Chem. B* 109 (2005) 7399–7406.
- [41] I.A. Weinstock, *Chem. Rev.* 98 (1998) 113–170.
- [42] R.R. Ozer, J.L. Ferry, *Environ. Sci. Technol.* 35 (2001) 3242–3246.
- [43] I.V. Kozhevnikov, *Russ. Chem. Rev.* 56 (1987) 811–825.
- [44] Anon., *CRC Handbook of Chemistry and Physics*, 77th ed., CRC Press, 1996.
- [45] D.T. Sawyer, J.S. Valentine, *Acc. Chem. Res.* 14 (1981) 393–400.